ISSN 3023-5669 Journal of Material Characterization and Applications, Vol. 2, No. 2, pp 110-118 (2024)
www.matcharappjournal.com
https://doi.org/10.5281/zenodo.13738140

OPTIMISATION OF THE OPTICAL BAND GAP OF AEROSOL ASSISTED CHEMICAL VAPOUR DEPOSITED SnS THIN FILM SEMICONDUCTOR

Thomas Ojonugwa Daniel

Department of Physics, Alex Ekwueme-Federal University Ndufu-Alike, Ikwo, Abakaliki, Ebonyi state, Nigeria
Email:danielojonugwathomas@gmail.com; ORCID ID: 0000-0002-5176-9181

Received 26 July 2024; revised 23 August 2024; accepted 27 August 2024

Abstract

The conductivity of a SnS semiconductor is impacted by the electron trap connected to the grain boundary, which hinders the attainment of the threshold voltage necessary for transistor functioning. On glass substrates, SnS thin films with thicknesses ranging from 0.2 to 0.40 μm were formed using aerosol assisted chemical vapour deposition. Utilizing energy dispersive X-ray spectroscopy, profilometry, X-ray diffractometer, and scanning electron microscopy, the optical band gap properties, composition, and microstructure of the SnS thin film were assessed. It was discovered that the Sn and S elements in SnS thin films altered in composition as the films' thickness increased. The increase in crystallites for thicker films may be the cause of the reduction in optical band gap with increasing film thickness. The SnS thin film's energy band gap decrease as a result of an increase in crystalline nature brought on by an increase in adsorption atom mobility with thickness.

Keywords: SnS, grain size, optical band gap

1. Introduction

The dielectric gate and semiconductor channel layer material determine a field effect transistor (FET) with high carrier concentration's and low operating voltage [1]. Only the modulation of electronic states in oxides, nitrides, organic semiconductors and carbon nanotubes has been observed in field-effect transistors. Tin (II) sulphide-based electric double-layer FET technology is intriguing for its innovative device performance [2–3].

Due to a paucity of research, SnS, a type P semiconductor with a carrier concentration of $1016cm^{-3}$ and a hole of 1.4 $cm^2V^{-1}s^{-1}$ mobility, has not been extensively studied for application in field-effect transistors [4]. Thus, SnS is a worthwhile semiconductor to evaluate the chalcogenide family's viability for the channel of a FET and to identify the ideal deposition settings that would give the necessary features for its application. One parameter of relevance is the film thickness, which depends on the film microstructure.

Controlling the film thickness is crucial in semiconductor processing because it affects the structure and optical band gap among other parameters, both of which are essential for identifying the

performance characteristics of a semiconductor [5]. Island-like voids and traps in SnS films impact charge carriers, optical band gap, electrical conductivity, and FET threshold voltage due to small grain grains acting as electron traps.

Aerosol-assisted chemical vapour deposition is the relevant deposition technique (AACVD). The comparative advantage of AACVD is the use of precursors with less volatility, which expands the range of molecules employed for thin film deposition.

Based on typical values from the literature, a thickness of 0.20-0.40 μm was chosen for the field effect transistor in order to optimize the band gap of SnS film for use in transparent field effect transistors.

2. Materials and method

The deposition and characterization of the SnS were performed using the method a previously reported in [5-6]. In the range of 200 to 1100 nm, UV-1800 SHIMADZU was utilized to measure optical transmittance and absorbance vs wavelength, with the exception of optical characteristics.
The absorption coefficient α is express in equation 1 where the parameters bear their usual meanings.

$$\alpha = 2.303\frac{A}{t} \quad (1)$$

The Eg of SnS was determined by drawing a straight line from the plots of $(\alpha hv)^2$ vs Eg to the $(\alpha hv)^2$=0 axis (Tauc plot), where the optical band gap is shown by the intersection point.

3. Results and discussion

3.1. Compositional analysis

The thickness of the as-deposited thin films is 0.20 μm, 0.25 μm, 0.30 μm, 0.35 μm, and 0.40 μm. The elemental composition of the SnS films is as provided in Table 1 which is same as reported in our previous work [5], and Figure 1 gives the spectrum of the SnS thin films as-deposited.

In SnS thin films, Sn and S were discovered to predominate.

In addition, films that could be connected to the substrate used for deposition were found to include trace amounts of sodium (Na), silicon (Si), calcium (Ca), chlorine (CI) and oxygen [7]. Table 1 demonstrated that as film thickness increased, so did the Sulphur content.

There is less Sulphur in films with lower thicknesses than those with higher thicknesses.

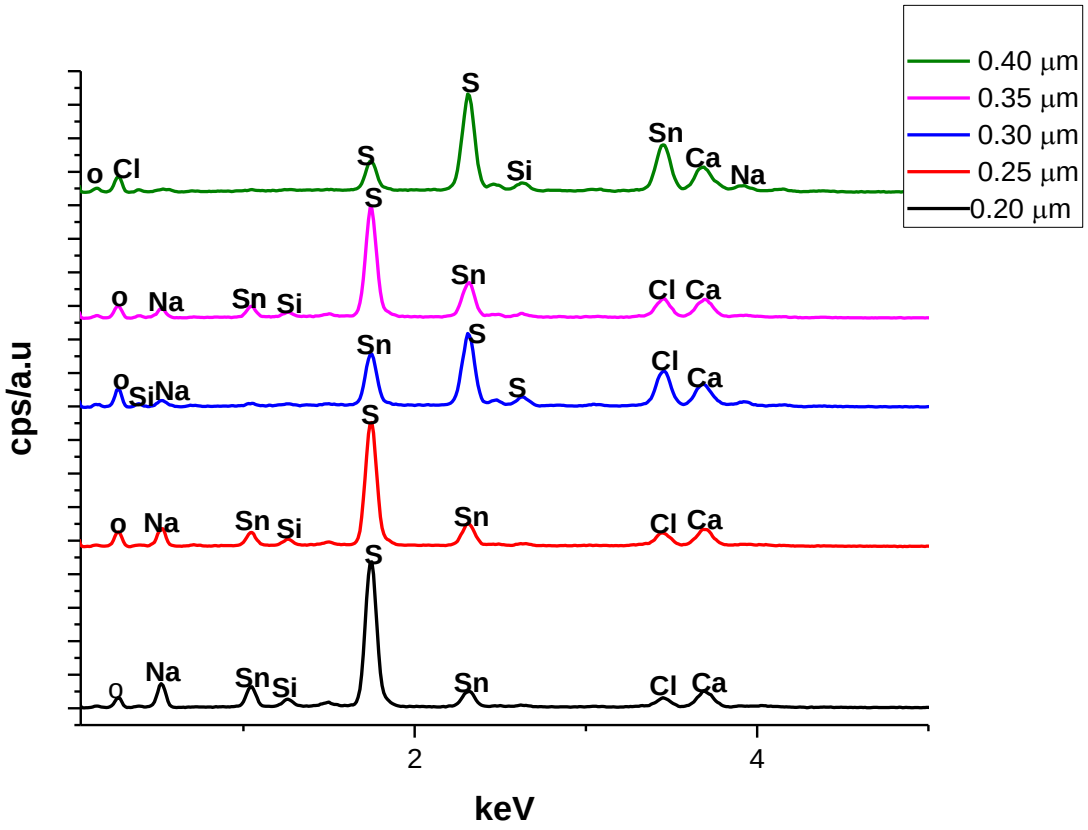

Fig. 1. EDS spectrum of the SnS thin films.

Table 1. As deposited SnS thin film composition in terms of atomic percent (at.%).

Thickness (μm)	Sn	S	Ca	Na	Cl	Si	O	TOTAL 100
0.20	36.43	45.57	8.35	1.04	5.62	1.74	1.25	100
0.25	35.72	46.28	8.35	1.04	5.62	1.74	1.25	100
0.30	33.19	48.81	8.35	1.04	5.62	1.74	1.25	100
0.35	30.75	51.25	8.35	1.04	5.62	1.74	1.25	100
0.40	29.85	52.15	8.35	1.04	5.62	1.74	1.25	100

As seen in Table 1, more sulphur atoms than tin atoms will land on the substrate because sulphur has a higher vapour pressure than tin. A lower sticking coefficient between the substrate surface and the film, caused by adsorbed-atom mobility, may be the reason for some of the sulphur atoms appearing to reflect back when they reach the substrate surface.

This would explain why there is a noticeable deficiency or lower sulphur content at a lower thickness in relation to a higher thickness.

Consistent with the report of [8], the effect diminishes at greater thicknesses due to a decrease in the scattering, which results in a decrease in thermal gradient with the clusters formation of the crystallites.

3.2. X-Ray Diffraction

Figure 2 show the XRD pattern of SnS thin films.

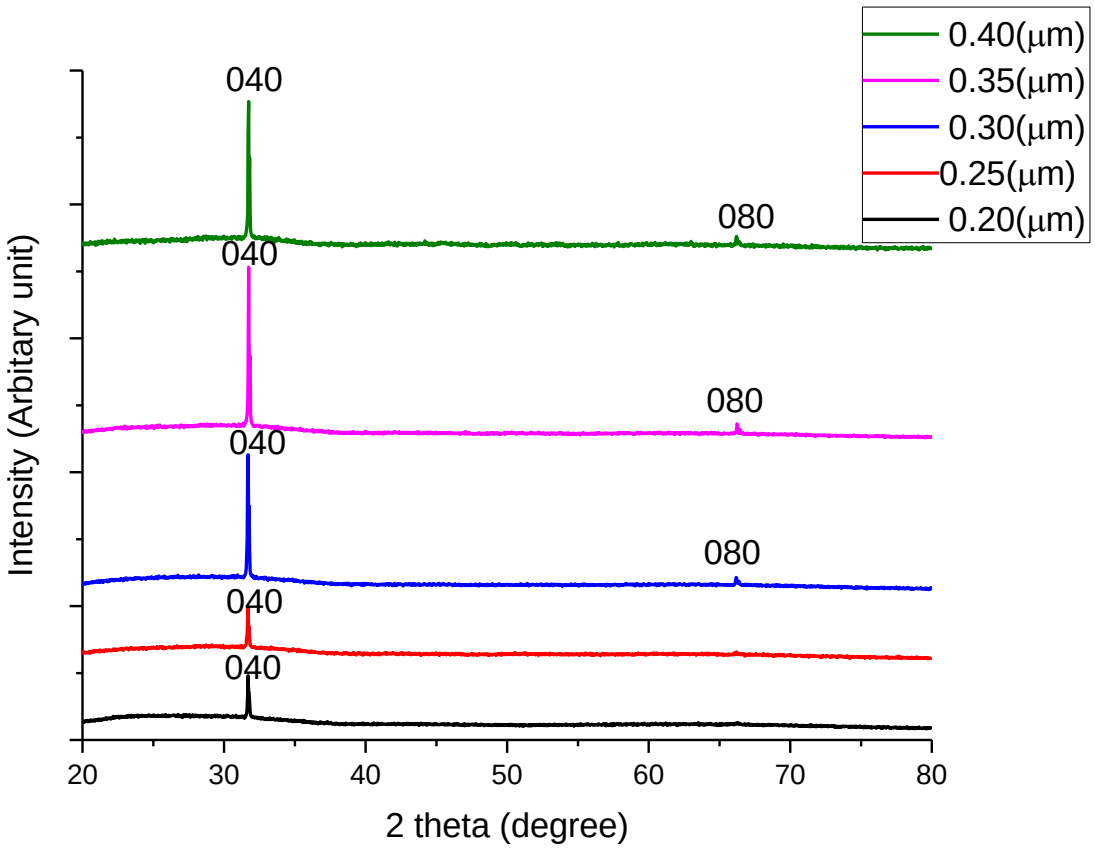

Fig. 2. XRD pattern for SnS thin films.

The pattern for herzenbergite was used to analyse and index the peaks identified for the films. The appearance of few peaks in the films' pattern analysis indicates the creation of a loosely pattern film. The films with thicknesses ranging from 0.2 to 0.25 μm exhibited a single peak diffracted along the (040) plane with a 2θ value of 31.7 °.

This peak may be the result of short-range atom ordering at the thickness level, allowing it to be seen as either a single crystal or a broad crystalline peak with suppressed other peaks.

The presence of few peaks could suggest that a low, crystalline, or amorphous thin film—a feature unique to chalcogenides formed at room temperature—is present at this thickness [9]. An increase in thickness does not cause a change in the film peak position, but it does cause an increase in intensity.

The amorphous network exhibits a unique broad peak, with increased film thickness enhancing crystallinity and narrower peaks. Table 2 provides structural parameters.

Table 2. Calculated structural parameters of SnS film.

S/n	Thickness (μm)	2Θ (°)	Full width half maximum β (°)	Grain size D (nm)	Dislocation density $\delta \times 10^{14}$ (Lines/m^2)	Micro strain $\varepsilon \times 10^{-4}$
1	0.40	31.73912	0.13633	60.57	2.73	5.72
2	0.35	31.74203	0.13935	59.26	2.85	5.84
3	0.30	31.75743	0.14260	57.94	2.98	5.99
4	0.25	31.70273	0.14629	56.44	3.14	6.13
5	0.20	31.70270	0.15030	54.94	3.31	6.30

The formation of atomic layers and thermal energy gain cause the crystallite size to increase with SnS film thickness, decreasing internal micro strain and flaws and ranging from 54.4 nm to 60.57 nm. Nuclide formation increases with increased film thickness due to decreased interactions between substrate and film layer.

Similar findings were reported in [5,6, 10–11]. By producing large film grains on the surface of smaller ones, a rise in film thickness causes the crystallite to enlarge [12-13].

The thickness of 0.40 μm may be the most crystalline since it has the biggest crystallite size. It is possible that stress release caused by the simultaneous growth phenomena, which improves film crystallinity with thickness.

3.3. Scanning electron microscopy (SEM)

SEM surface morphology of SnS thin films μm is shown in Figure 3.

Thicknesses ranging from 0.2 to 0.4 μm in SnS films display unique microstructures, such as agglomerates and well-defined grains. Low morphology, irregular surface, and porous grain growth occurs with increase in thickness.

Stronger interatomic interactions in deeper layers provide a tight grain structure as film thickness rises, whereas weaker interatomic forces in surface atoms produce a loosely packed grain structure [9, 12].

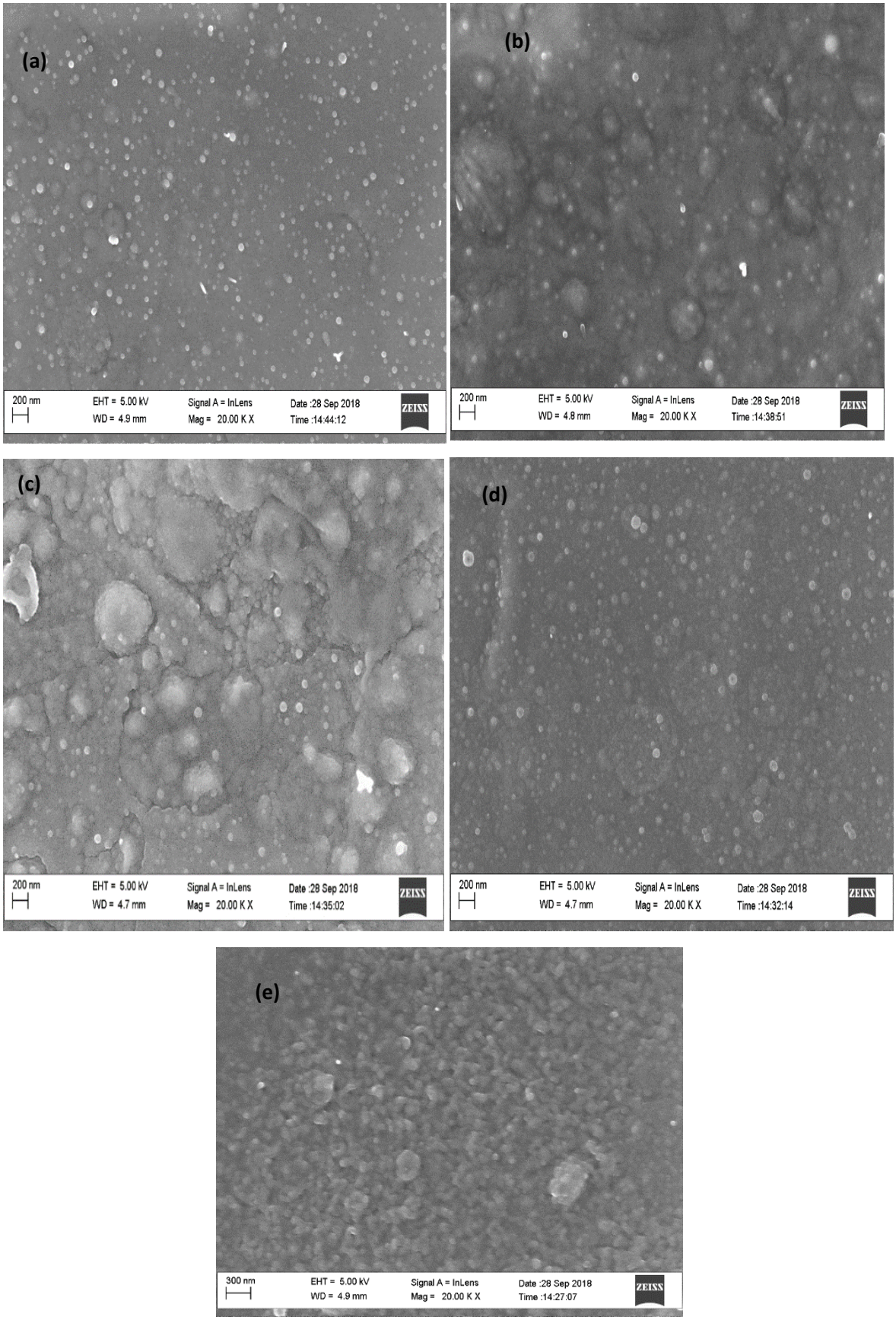

Fig. 3 (a-e). The surface morphology of films of 0.2(a), 0.25(b), 0.30(c), 0.35(d) and 0.40(e) μm.

The film thickness increases grain size, attributed to coalescence in the tightly packed film grain size.

3.4 Optical Energy Band Gap of Varied Film Thickness and Annealing Temperature

Tauc plots of SnS films are shown in Figure 4(a-e), which estimate the band gap.

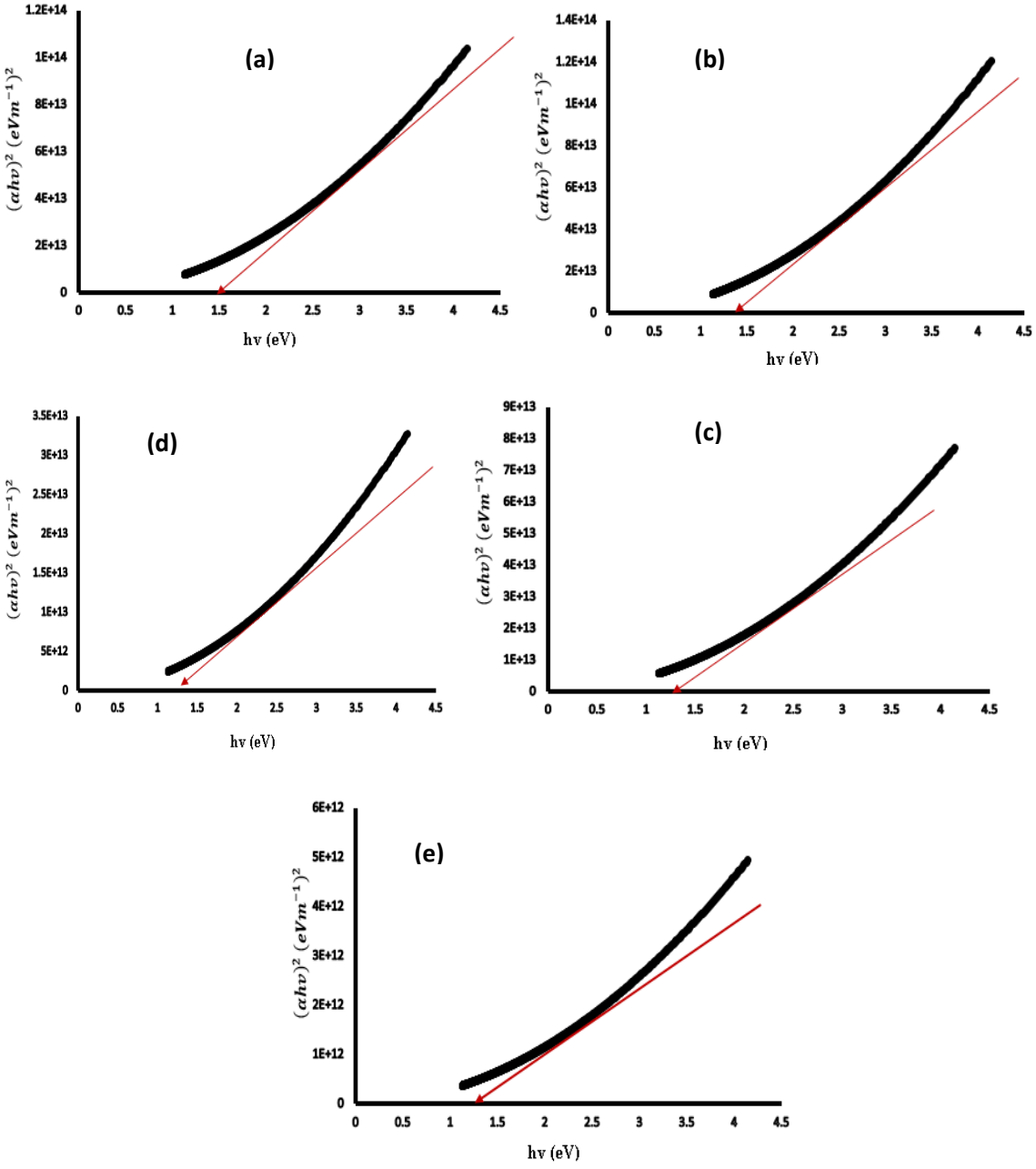

Fig. 4. (a-e).Tauc plots for 0.20, 0.25, 0.30,350 and 0.40 μm.

SnS thin films of varying thicknesses have a linear relationship in the optical band gap, which represents the energy needed to drive an electron to the conduction band and suggests that these films are direct transitions.

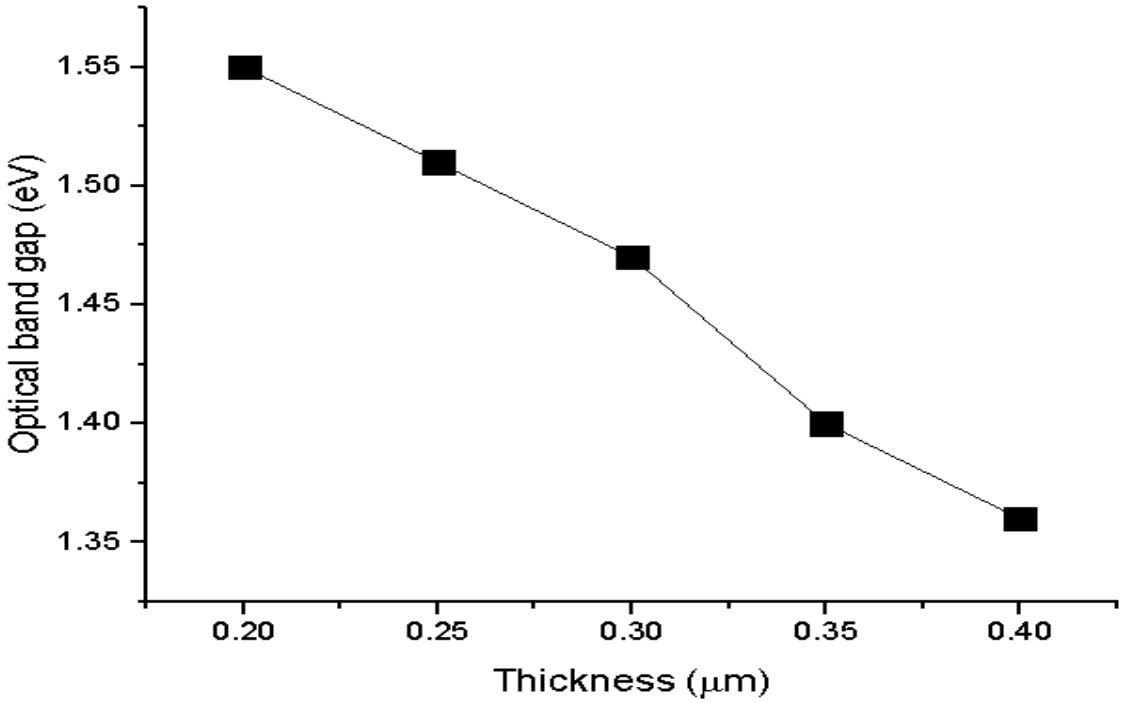

Fig. 5. Variation of optical band gap of SnS thin films.

Based on Figure 5, the band gap decreased from 1.55 eV for 0.20 μm to 1.36 eV for 0.40 μm. The XRD results indicate that a substantial density of dislocation and an increase in grain size leads to the decrease in band gap that occurs as thickness increases. There have also been reports of a decline in the band gap with increasing thickness [14–15]. It has been observed that films, such as those with thicknesses of 0.2, 0.25, and 0.30 m, frequently cause greater transmission range, causing the absorption edge to move to a shorter wavelength and, as a result, producing a bigger band gap [16]. The increase in crystallite size may be the cause of the decrease in optical band gap with increasing thickness. As thickness grows, so does the mobility of the adsorption atoms, leading to a corresponding increase in crystalline and a subsequent decrease in the energy band gap [17]. Another, explanation for the drop in Eg with thickness is the rise in the localized states close to the band, which similarly lowers the value of Eg [18].

Most semiconductors used in field effect transistors, such as silicon, have Eg between 1.0 and 1.5 eV, allowing for low voltage operation. In contrast, wide-band gap materials, like gallium and aluminium nitride, have band gaps between 2-4 eV, allowing for much higher temperatures, frequencies, and voltages of operation than those of conventional semiconductor materials. The energy band gap value, optimum at 1.36 eV, is suitable for a semiconductor's performance in an EDLFET at a low voltage range of 0 to ±3V.

4. Conclusion

It was discovered that the SnS thin film produced by AACVD was polycrystalline, with different compositions of Sn and S elements. Large grain sizes cause the grains and trap density to decrease as the SnS thickness increases from 0.20μm to 0.40μm. Grain size and boundary effect determine the semiconductor optical band gap, which is directly proportional to the transistor's threshold voltage.

The crystallinity of the film increases with thickness due to an increase in adsorption atom mobility, which causes the energy band gap to reduce. suggests that SnS thin film may be used or used as a channel layer semiconductor in a FET.

References

[1] H. Du, X. Lin, Z. Xu, and D. Chu, Electric double layer field effect transistors: a review of recent progress, J. Mater. Sci. **50**(17), 095095 (2015).

[2] H. Yuan, H. Liu, and H. Shimotani, Liquid gated ambipolar transport in ultrathin films of a topological insulator Bi_2Te_3, Nano Lett. **11**(7), 2601-2605 (2011).

[3] P. Thiruramanathan, G. S. Hikku, R. Krishna-Sharman, and M. S. Shakthi, Preparation and characterisation of indium doped SnS thin films for solar cell applications, Int. J. Technochem. Res. **1**(1), 59-65 (2015).

[4] S. S. Hedge, A. G. Kunjomana, K. A. Chandrasekharam, K. Ramesh, and M. Prashantha, Optical and electrical properties of SnS semiconductor crystals grown by physical vapour deposition technique, Physica B **406**(5), 1143-1148 (2011).

[5] T. O. Daniel, U. E. Uno, K. U. Isah, and U. Ahmadu, Optimization of electrical conductivity of SnS thin film of $0.2< t\leq 0.4$ μm thickness for field effect transistor application, Rev. Mex. Fis. **67**(2), 263-268 (2021).

[6] T. O. Daniel, U. E. Uno, K. U. Isah, and U. Ahmadu, Tuning of SnS thin film conductivity on annealing in an open air environment for transistor application, East Eur. J. Phys. **2**, 94-103 (2020).

[7] A. Sugaki, A. Kitakaze, and H. Kitazawa, Synthesized tin and tin-sulfide minerals; synthetic sulfide minerals (XIII), Sci. Rep. Tohoku Univ. **16**(2), 199-211 (1985).

[8] A. Gomez, H. Martinez, M. Calixto-Rodriguez, D. Avellaneda, P. G. Reyes, and O. Flores, A study of the structural, optical and electrical properties of SnS thin films modified by Plasma, J. Mater. Sci. Eng. **3**(6), 352-358 (2013).

[9] P. Prathap, N. Revathi, S. Subbaiah, and K. T. R. Reddy, Thickess effect on the microstructure, morphology and optoelectronic properties of ZnS films, J. Phys.: Condens. Matter **20**(3), 035205-035215 (2008).

[10] P. Jain and A. P. Arun, Parameters influencing the optical properties of SnS thin films, J. Semicond. **34**(9), 1-6 (2013).

[11] M. Devika, N. R. Koteeswara, K. R. Gunasekhar, E. S. R. Gopal, and R. K. T. Ramakrishna, Influence of annealing on the physical properties of evaporated SnS films, Semiconductor Science and Technology **21**, 1125-1131 (2006).

[12] A. U. Moreh, M. Momoh, H. N. Yahaya, B. Hamza, I. G. Saidu, and S. Abdullahi, Effect of thickness on structural and electrical properties of $CuAlS_2$ thin films grown by two stage vacuum thermal evaporation technique, Int. J. Math. Comput. Phys. Comput. Eng. **8**(7), 1084-1088 (2014).

[13] A. Jain, P. Sagar, and R. M. Mehra, Changes of structural, optical and electrical properties of sol-gel derived ZnO films with their thickness, Mater. Sci. Pol. **25**(1), 233-242 (2007).

[14] W. S. Rasband, ImageJ, National Institute of Health, Bethesda, Maryland, USA, 1997-2014.

[15] O. E. Ogah, G. Zoppi, I. Forbes, and R. W. Miles**,** Thin films of SnS for use in thin film solar cell devices, Thin Solid Films **517**(7), 2485-2488 (2009).

[16] T. H. Patel, Influence of deposition time on the structural and optical properties of chemically deposited SnS thin films, The Open Surface Science Journal **6**, 6-13 (2012).

[17] A. Tumuluri, K. L. Naidu, and K. C. J. Raju, Band gap determination using Tauc's plot for $LiNbO_3$ thin films, Int. J. Chem. Tech. Res. **6**(6), 3353-3356 (2014).

[18] E. Guneri, C. Ulutas, F. Kirmizigul, G. Altindemir, F. Gode, and C. Gumus, Effect of deposition time on structural, electrical and optical properties of SnS thin films deposited by chemical bath deposition, Appl. Surf. Sci. **257**(4), 1189-1195 (2010).